Asian Power Electronics Journal, Vol. 13, No. 2, October 2019

A Simple and Useful Three-Port Converter for Integrating Renewable Energy Sources in Stand-Alone Systems

Chen M. X Ho F. H Cheng K. W. E

Abstract−A simple and useful three-port converter is proposed in this paper, which is suitable for integrating renewable energy sources in off-grid applications with low to medium power. It mainly consists of a coupled inductor and two active switches. Isolation between the two renewable energy sources is achieved. Only one active switch functions in either loading mode or battery-charge mode. Hence the switching losses is reduced. Output diode of the proposed converter is removable from the system if one of the power source is integrated inside with anti-reversed-current diode, so that the system overall cost is reduced. Easy control techniques can be applied to the converter, since power decoupling control is not necessary due to out power constraint of a single PV panel. A 110*W* prototype was built and tested under loading mode and battery-charge mode to validate the theoretical analysis. Active snubber to eliminate voltage spike on the switches is introduced and results shown that zero-voltage switching (ZVS) is achieved.

Keywords−Three-port converter, less component count, simple control strategies

I. INTRODUCTION

Nowadays, due to the energy crisis and the side effects of burning fossil fuel, such as rapid growth of green-house gases (GHGs), global warming and rising sea level, it poses a threat to the existence of human beings. In order to deal with these problems, renewable energy sources (solar, wind, fuel cell) offer a good solution. Among these clean energies, solar is regarded as the most promising one. From satellite, electric vehicle (EV) to street lamp, the usage of photovoltaic or PV has fully penetrated the modern society [1]. Especially in stand-alone systems, it is very easy to harvest solar energy and transfer into electricity for off-grid applications (Fig. 1).

As it is known that the output voltage of a PV panel is variable and usually range from 20V to 40V (Fig. 2). Traditional way of using the solar energy in off-grid system is that a DC-DC converter is adopted to provide a constant output voltage which charges the battery. Thus, energy is captured and preserved for future usage when it is needed by discharging the battery. In this case, another DC-DC converter is also required to provide a regulated voltage for the load (motor, LED, etc) as shown in Fig. 3(a).

Recently, three-port converter (TPC) has become a popular topic in the application for renewable energies (Fig. 3(b)). It can provide an easy integration of multiple energy sources through a single converter, making energy transferred process more efficient compared with the traditional way of two-stage power transfer [2]. TPC with large DC gain are also discussed by many previous publications [3-5]. With high output voltage, they can provide suitable interfaces as the front-end to the renewable energy sources for on-grid applications [4]. However, power decoupling control is required where there is single-input-multiple-output (SIMO) operation mode [6]. Sometimes, additional active switches must be used to regulate the output voltages. However, not all applications require SIMO operation mode, such as in small electrical vessel systems or school shuttles. Due to the limited space, only one PV panel is allowed to be installed on the vessel. Other power sources such as battery is also included to ensure enough power for motor driving. Energy from solar panel is incapable to charge the battery and supplies the load at the same time. Under this constraint, available solutions for TPCs that containing SIMO (PV supplies output and charges battery simultaneously) is over design. Moreover, decoupling control for them is needed to regulate the output voltages, which will make the whole system more complex and less cost-effective.

In this paper, a simple TPC based on a coupled inductor is proposed to integrate the PV and battery in stand-alone system operating at medium power level (Fig. 4). Its features are as follows.

1) less component count: a coupled inductor, two active switches, one (or two) diode(s), two capacitors (including the output capacitor).
2) partly isolation: isolation between two power sources.
3) easy control and driving scheme: duty cycle control to regulate output voltage.
4) relatively high output voltage and low voltage stress.

The proposed TPC is cost-efficient because while components in the two-stage power converters have only one function, most components in the proposed TPC have multiple functions so that they can be shared in different modes, minimizing overall cost. Moreover, the relatively high output voltage reduces the number of the battery cells required in stand-alone systems. The proposed converter simplifies the power-transfer process compared with two-stage power conversion and increases the system efficiency. In the aforementioned-applications, (mostly in stand-alone systems with low to medium power rating) with input power constraint, without considering the decoupling control, simple control strategies can be applied. For easy understanding, the proposed converter is divided into two operation modes named as “loading mode” and “battery-charge mode”, and single PV panel and battery cells are considered as the renewable power sources.

In loading mode, the PV panel together with the battery supplies the load through the proposed TPC. Under extreme scenarios such as bad weather, the PV panel is by-passed by a diode and only the battery acts as the power source.

Battery-charge mode usually begins when the load is detached from the system (for example, the vessel stops).

Power Electronics Research Centre, Department of Electrical Engineering, The Hong Kong Polytechnic University, Hong Kong
E-mail: mxchen@polyu.edu.hk

The generated power from the PV is installed in the battery by charging it through the TPC. In this mode, switch S_1 is turned off, however, its body diode is still functioning to form a charge loop. If the charge current is large, it is recommended to place a diode D_a in parallel with the body diode to reduce the conduction losses (Fig. 4 (b)).

The two operation modes of the proposed TPC are illustrated in detail below. The following assumptions are considered.

1) leakage inductance of coupled inductor is neglected, and turns ratio of the coupled inductor is $N_p : N_s = 1 : n$.
2) capacitors are large enough so that the voltages across them are treated as constant.
3) all the components are in ideal state. i.e. parasitic resistance is neglected.

(a) (b)

Fig. 1: PV application for small vessel. (a) Single PV panel consisting 72 cells (36V open circuit voltage). (b) Electrical vessel integrating with a PV panel and battery as power sources.

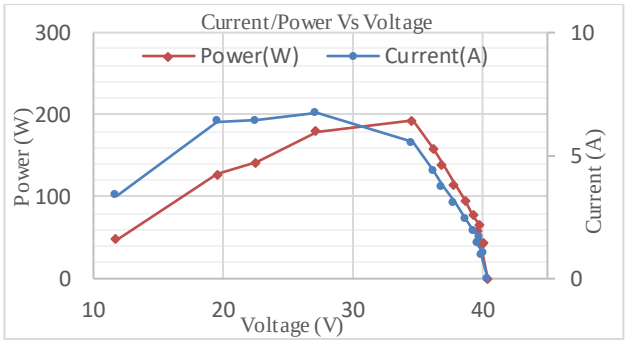

Fig.2: V/I characteristics and power output of a PV panel.

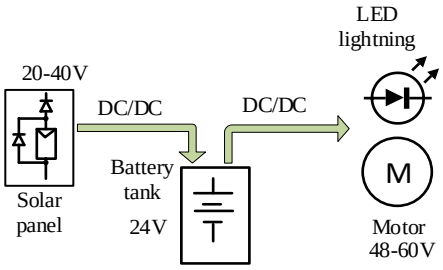

(a)

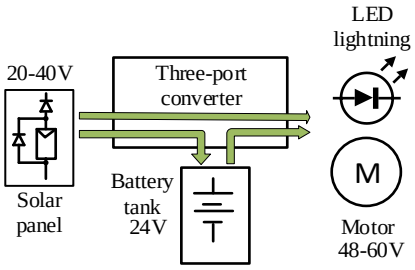

(b)

Fig. 3: Two ways of preserving and using the renewable energy. (a) Traditional way of two-stage energy conversion. (b) Another way of using three-port converter.

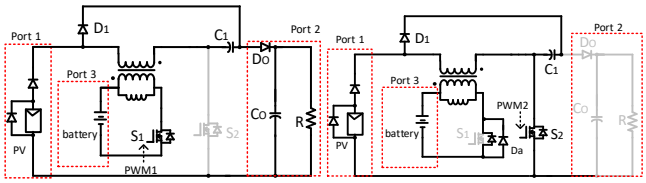

Fig. 4: Proposed TPC for off-grid application. (a) Loading mode. (b) Battery-charge mode

II. Loading Mode Analysis of the Proposed TPC

In this mode, the load is connected to the converter. Both the PV and battery supply the load through a TPC. PV cannot charge the battery in this mode due to limited power. Switch S_2 is turned off at all time. Gating signal PWM1 drives S_1. The wingding connected in series with battery act as the primary side of the coupled inductor while the other wingding act as the secondary side. For easy understanding, leakage inductance of the coupled inductor is neglected. There are two switching stages for S_1 in this mode. Assume switching frequency of PWM1 driving signal is $f_s = \frac{1}{T}$, with duty cycle D_1. The two switching stages are illustrated in Fig. 5 (a, b).

Stage 1) switch on $(0 < t < D_1 T)$ (Fig. 5 (a)): during this stage, the main switch S_1 is turned on. Current from battery flowing through primary side of coupled inductor, main switch and then back to the battery. At the same time, the magnetizing inductor L_m is getting charged by the battery voltage, with its current increases linearly.

$$i_{Lm} = \frac{V_{Lm}}{L_m} DT \quad (1)$$

$$V_{Lm} = V_b \quad (2)$$

where V_{Lm} is the voltage across the primary side of coupled inductor. In the secondary side, current flowing out of PV panel, going through secondary side of coupled inductor, capacitor C_1 and then supplies the load. Energy stored in the capacitor C_1 discharges to the output, further stepping up the output voltage. Equations can be written

$$V_{pv} + V_s + V_{c1} = V_o \quad (3)$$

$$V_s = nV_{Lm} = nV_b \quad (4)$$

where V_s is the voltage across the secondary side inductor.

This stage ends when the main switched is turned off and begins the next stage.

Stage 2) switch off ($D_1T < t < T$) (Fig. 5 (b)): in this stage, the main switch S_1 is turned off. Energy stored in the magnetizing inductor discharges to the secondary side through magnetic coupling. The output diode of PV panel is reversed biased, protecting PV from being damaged by the reversed current. Capacitor C_1 is getting charged by the voltage across the secondary side inductor. Output diode is reversed biased as well. And the output capacitor supplies the output, keeping a constant output voltage. Equations can be written in this stage

$$V_s = nV_{Lm} \quad (5)$$
$$V_s + V_{c1} = 0 \quad (6)$$

Of the two stages in loading mode, voltage-second balance is applied to the magnetizing inductor.

$$V_b D_1 T - \frac{V_{C1}}{n}(1 - D_1)T = 0 \quad (7)$$

By substituting equation (4) into (6), one can find the capacitor voltage V_{c1} is

$$V_{c1} = \frac{nD_1}{1-D_1} V_b \quad (8)$$

And the DC gain of the TPC is

$$\mathrm{M} = \frac{n}{1-D_1} V_b + V_{pv} \quad (9)$$

Relatively high output voltage is obtained, which means the number of onboard battery cell can be reduced. And regulated output voltage is achieved by duty cycle control applied to PWM1.

The voltage stress on the switch S_1 and the diode D_1 are also found

$$V_{ds1} = \frac{1}{1-D_1} V_b \quad (18)$$
$$V_{d1} = \frac{n}{1-D_1} V_b \quad (19)$$

Low voltage stress on semiconductor devices which facilitate the use of switch with low on-resistor (R_{ds_on}).

Average output current for the battery is calculated as follows.

$$\int_0^T I_b = \int_0^{DT} (I_p + I_{Lm}) dt \quad (10)$$

where I_p is the average current flowing through primary side of coupled inductor and I_{Lm} is the average magnetizing inductor current. They are represented as

$$\int_0^{DT} I_p \, dt = \int_0^{DT} nI_s \, dt = \int_0^{DT} nI_o \, dt \quad (11)$$
$$I_p = nI_o \quad (12)$$

Current-balance on capacitor C_1 yields

$$\int_{DT}^T I_{C1} = \int_0^{DT} I_o \quad (13)$$

where I_{C1} is the average current of capacitor C_1 in switching stage stage 2. one can get

$$\int_{DT}^T I_{Lm} \, dt = \int_{DT}^T nI_{C1} \, dt \quad (14)$$
$$I_{Lm} = \frac{nD}{1-D} I_o \quad (15)$$

By substituting equations (12, 15) into (10), yields

$$I_b = \frac{n}{1-D} I_o \quad (16)$$

From Fig. 5 (a), one can get the average current for PV output is

$$I_{pv} = I_o \quad (17)$$

As the PV output diode and the converter output diode D_o are both turned off at this stage, and they are in series connected in a loop. Voltage stress on the two diodes are

$$V_{do} = V_{dpv} = \frac{1}{2}(V_o - V_{pv}) = \frac{n}{2(1-D_1)} V_b \quad (20)$$

One may easily find that one of these two diodes is redundant and can be discarded. In practical cases, almost every PV panel is integrated inside with an output diode to prevent reversed current. So that the output diode D_o is free to remove from the converter in applications where the overall system cost is a critical factor determining the converter design, provided that the voltage stress on output diode of PV panel isn't over the rated value. By doing so, the overall system cost is reduced, and the power conversion efficiency is expected to increase. Both two diodes are preserved in the above analysis and their voltage stress are halved compared with reduced-diode version. The key waveforms of the proposed TPC in loading mode is shown in Fig. 6.

It should be noted that there are two extreme scenarios in this mode. When sun irradiation is very low under bad weather, PV panel is bypassed by the bypass diode. The DC gain becomes

$$\mathrm{M} = \frac{n}{1-D_1} V_b \quad (21)$$

And higher duty cycle is applied to compensate for the loss of V_{pv} (Fig. 7 (a)). When the battery is damaged or removed, PV may supply the load under some specific circumstances (Although it is not good to have the load running under rated power, it may be life-rescuing to drive the vessel back by using PV power source). In this case the TPC becomes a common DC converter whose output is

$$V_o = \frac{2-D_2}{1-D_2} V_{pv} \quad (22)$$

where D_2 is the duty cycle of switch S_2.

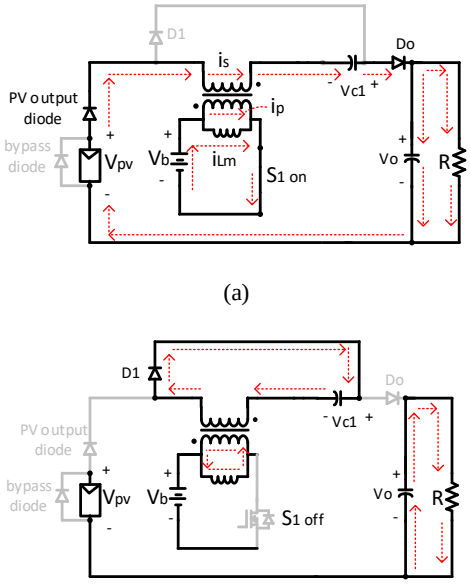

Fig. 5: Two switching stages of loading mode. (a) Switch S_1 on. (b) Switch S_1 off.

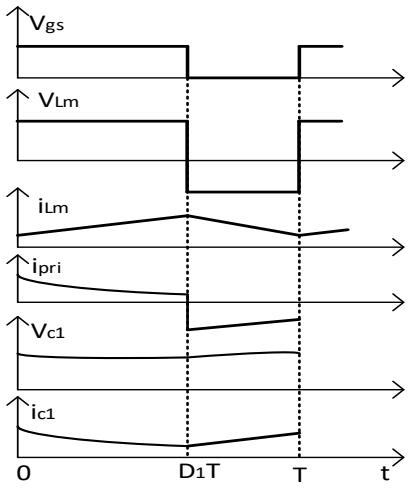

Fig. 6: Key waveforms of the proposed TPC in loading mode.

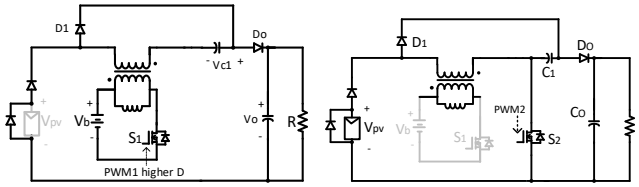

Fig.7: Two extreme scenarios in loading mode. (a) PV panel is bypassed. (b) Battery doesn't work.

III. Battery-Charge Mode Analysis of The Proposed TPC

In this mode, the load is detached from the converter (Fig. 8 (a, b)). For an example, when the vessel stops running. Main switch S_1 is turned off all the time, while S_2 is turned on periodically. Body diode of S_1 still conducts in this mode. Additional diode can be placed in parallel to the body diode in high-power applications with high current. The wingding in series with PV acts as the primary side of the coupled inductor. The battery which stores the energy from PV panel is the load in this mode. Although diode D_1 remains, it is reversed biased all the time. Actually, the TPC becomes a fly-back converter in this mode. Results are given out here directly. The battery-charge voltage is regulated by the duty cycle D_2 of the driving signal PWM2.

$$V_b = \frac{n D_2}{1-D_2} V_{pv} \tag{23}$$

And the voltage stress on switch S_2 is

$$V_{ds2} = \frac{1}{1-D_2} V_{pv} \tag{24}$$

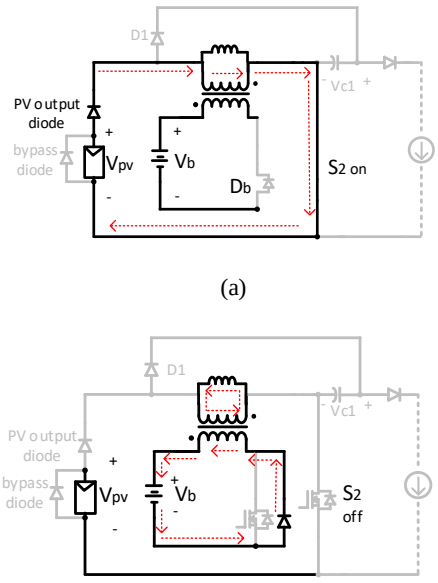

Fig. 8: Switching stages in battery-charge mode. (a) Switch on. (b) Switch off.

It should be noted that in this mode, energy generated by PV panel is used to charge battery only. The output cannot be supplied by the PV in this mode due to the lower power level. This is the difference between the proposed TPC and the available TPCs [1-6]. Instead, the converter changes to loading mode with double inputs when it is needed to supply the load.

IV. Design Considerations

1. Coupled inductor design

Consider that most of the PV output voltage V_{pv} is in the range of 20-40V (30V nominal output), and the 24V battery cells are very common. Based on equation (15), the turns ratio of the coupled inductor is selected as n = 1.

In loading mode, apply current balance equation on capacitor C_1, one can find

$$I_o \times D_1 = I_{D1} \times (1 - D_1) \tag{25}$$

$$I_{D1} = I_{Lm} \tag{26}$$

where I_{D1} and I_{Lm} are the average current flowing through diode D_1 and the magnetizing inductor in Fig. 5 (b)

respectively. So the average current of magnetizing inductor can be expressed

$$I_{Lm} = \frac{D_1}{1-D_1} I_o \tag{27}$$

To ensure that the converter works at CCM and guarantee a good efficiency, 10% of current ripple for the magnetizing inductor is considered. Thus the magnetizing inductance should be calculated as

$$L_m = \frac{2V_b D_1 T}{10\%\ I_{Lm}} \tag{28}$$

Once the magnetic core is selected, the numbers of turns for primary and secondary side are found.

In battery-charge mode, similar method is used to find L_m. L_m calculated in both modes are taken into consideration and the larger one is chosen for design.

2. semiconductor component design.
In loading mode, voltage stress for switch and diodes are found from equations (10-12).

The average current flowing through the switch S1 is

$$I_{ds} = I_{Lm} + I_p = \frac{1}{1-D_1} I_o \tag{29}$$

And its RMS value is

$$I_{ds\_rms} = I_{ds}\sqrt{D_1} \tag{30}$$

The average current flowing through output diode is I_o (smaller values for the other average diode currents). Similar method is applied to batter charge mode and a comparative selection of the semiconductor components should be made.

V. Simulation and Experimental Results

1. Simulation Results
The proposed converter is simulated by PSIM. Gating signal PWM1 is 100 kHz with 0.5 duty ratio. PV voltage is set to 30V and battery voltage is set to 24V in loading mode. Simulation results are shown in Figs. 9-10. Without adding voltage clamp circuit to the switch, a voltage spike is found in V_{ds1} immediately after the switched turned off. The average output current of the PV is half of the battery's which matches with theoretical results in equation (16-17). In battery-charge mode, similar voltage spike is tested on the switch S_2. A constant output voltage is achieved to charge battery.

2. Experimental Validation.
To further examine the proposed converter, a prototype was built and tested. Configurations for the prototype are as follows.

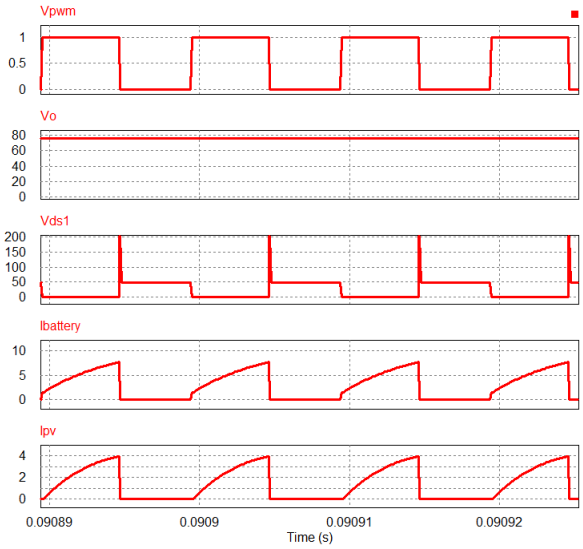

Fig. 9: Simulation results in loading mode with double inputs. Gating signal V_{pwm}; output voltage V_o; voltage stress on switch S_1, V_{ds1}; two input currents I_{pv} and $I_{battary}$.

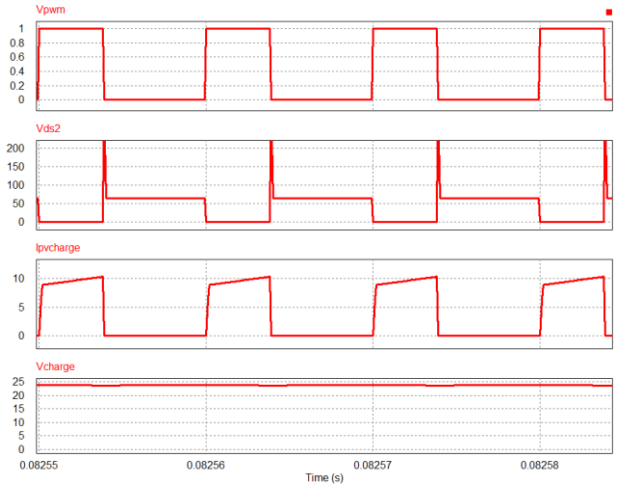

Fig. 10: Simulation results in battery-charge mode. gating signal V_{pwm}; battery-charge voltage V_{charge}; input currents $I_{pvcharge}$; voltage stress on switch S_1, V_{ds1}.

Table I: Configurations for the Proposed Converter

Input voltage	$V_{pv} = 30V$, $V_b = 24V$
Output voltage	$V_o = 68V, 100\ W$
Switches S_1, S_2	$FDPF51N25$ (250V,51A, $R_{ds_{on}} = 0.06\Omega$)
Diodes D_1, D_o	$60EPU02PbF$ (200V, 60A)
Coupled inductor	$L_m = 122u, L_k = 1.3u.$
Capacitors C_1, C_o	100V,200uF (ESR 0.05 Ω)

The experimental results are shown in Figs. 11-12. Similar to the simulation results, voltage spike on switch is. It may also bring larger voltage ripple to the output in batter-charge mode.

3. Improved Performances test
To improve the converter performances, two active snubbers are added at the primary and secondary sides of the coupled inductor to eliminate voltage spike on the switches. L-C filter to minimize the output current ripple of PV panel is also added. Zero-voltage switching (ZVS) is achieved by the switches.

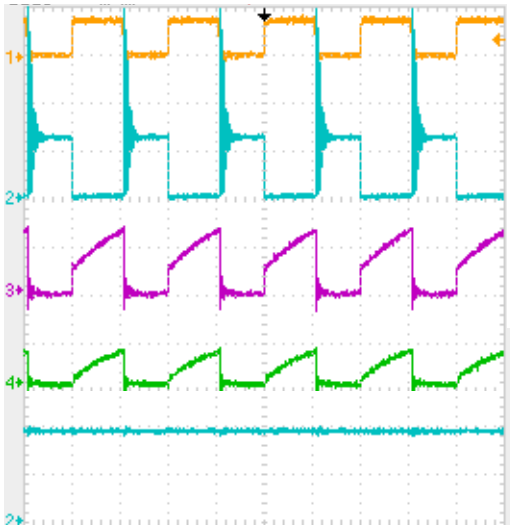

Fig. 11: Experimental results in loading mode with double inputs. Gating signal V_{pwm}; output voltage V_o $(40V/div)$; voltage stress on switch S_1 , V_{ds1} $(40V/div)$; two input currents I_{pv} $(5A/div)$ and $I_{battary}$ $(5A/div)$.

Fig. 12: Experimental results in battery-charge mode. gating signal V_{pwm}; battery-charge voltage V_{charge} $(10V/div)$; input currents $I_{pvcharge}$ $(5A/div)$; voltage stress on switch S_1, V_{ds1} $(40V/div)$.

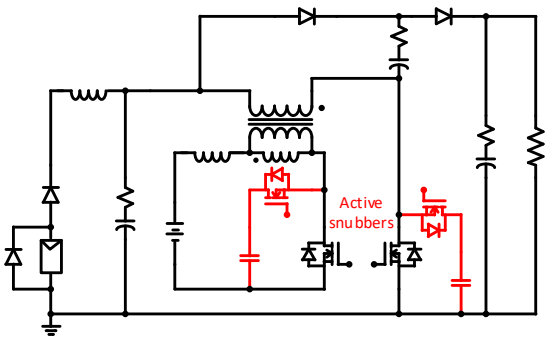

Fig. 13: Including active snubber to clamp voltage on switch.

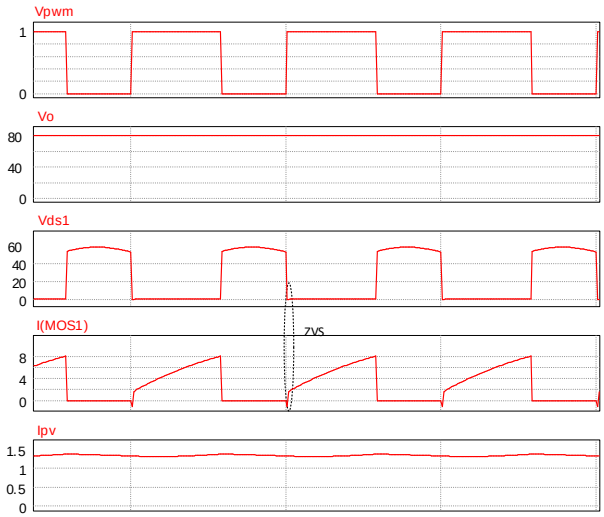

Fig. 14: Simulation results in loading mode with double inputs. Gating signal V_{pwm}; output voltage V_o; voltage stress on switch S_1, V_{ds1}; two input currents I_{pv} and $I_{battary}$.

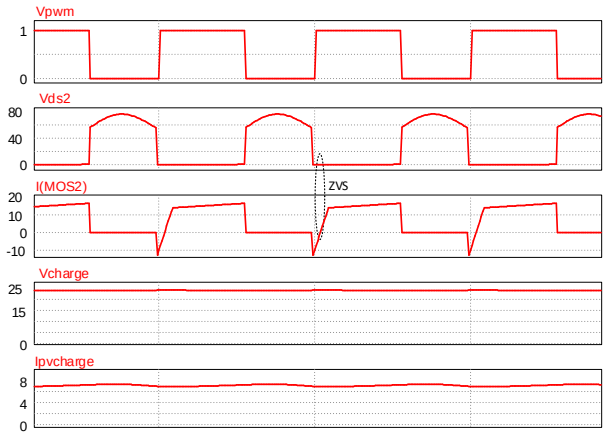

Fig. 15: Simulation results in battery-charge mode. gating signal V_{pwm}; battery-charge voltage V_{charge}; input currents $I_{pvcharge}$; voltage stress on switch S_1, V_{ds1}.

VI. Conclusions and Future Discussions

A very simple and useful three-port converter (TPC) is proposed. The proposed converter uses less power devices such as Mosfet or diode but provides an easy integration for multiple renewable energies sources. In loading mode and batter-charge mode, the output voltage is regulated by duty cycle of the switch signals D_1 and D_2, no complex control required. The converter with active clamp circuit to deal with the leakage inductance is simulated and results show that ZVS is achieved. Yet, the cost of the system is increased. So a trade-off between converter cost and the power transfer efficiency exists when designing the proposed TPC.

References

[1] J. P. Benner and L. Kazmerski, “Photovoltaics gaining greater visibility,” IEEE Spectr., vol. 29, no. 9, pp. 34–42, Sep. 1999.

[2] N. Zhang, D. Sutanto, K. M. Muttaqi, “A review of topologies of three-port DC–DC converters for the integration of renewable energy and energy storage system,” *Renewable and Sustainable Energy Reviews*, 56 (2016) 388–401.

[3] Y. Chen, A. Q. Huang and X. Yu, “A High Step-Up Three-Port

DC–DC Converter for Stand-Alone PV/Battery Power Systems," *IEEE Trans. Power Electron.*, vol. 28, no. 11, pp. 5049-5062, Nov. 2013.

[4] L. Chien, C. Chen, J. Chen and Y. Hsieh, "Novel Three-Port Converter with High-Voltage Gain," *IEEE Trans. Power Electron.*, vol. 29, no. 9, pp. 4693-4703, Sept. 2014.

[5] H. Wu, K. Sun, R. Chen, H. Hu, and Y. Xing, "Full-Bridge Three-Port Converters with Wide Input Voltage Range for Renewable Power Systems," *IEEE Trans. Power Electron.*, vol. 27, no. 9, pp. 3965-3974, Sept. 2012.

[6] C. Zhao, S. Round and J. Kolar, "An Isolated Three-Port Bidirectional DC-DC Converter with Decoupled Power Flow Management," *IEEE Trans. Power Electron.*, vol. 23, no. 5, pp. 2443-2453, Sept. 2008.